ELSEVIER

Coordination Chemistry Reviews
185–186 (1999) 403–416

COORDINATION CHEMISTRY REVIEWS

Artificial photosynthesis in lamellar assemblies of metal poly(pyridyl) complexes and metalloporphyrins

David M. Kaschak, Stacy A. Johnson, Chad C. Waraksa, Jessica Pogue, Thomas E. Mallouk *

Department of Chemistry, The Pennsylvania State University, University Park, PA 18602, USA

Contents

Abstract

Multilayer films composed of inorganic colloids (α-zirconium phosphate or $HTiNbO_5$) and organic polycations can be grown in almost any desired sequence on surfaces by electrostatic self-assembly. Control of the edge chemistry of the anionic sheets is essential to the preparation of well organized monolayers and multilayers. Examples are given of layer sequences that incorporate electron donors and acceptors, which undergo photoinduced electron transfer reactions across inorganic spacer layers. Similar stacking sequences can be used to couple light harvesting assemblies, containing energy donors and acceptors, to electron donor-acceptor dyads.

* Corresponding author. Tel.: +1-814-863-9637; fax: +1-814-863-8403.
E-mail address: tom@chem.psu.edu (T.E. Mallouk)

0010-8545/99/$ - see front matter
PII: S0010-8545(99)00025-9

Keywords: Photochemistry; Electron transfer; Energy transfer; Supramolecular chemistry; Self-assembly

1. Introduction

One of the interesting challenges facing materials chemists today is the control of structure on the supramolecular length scale, which is in the regime of nanometers to microns. For artificial photosynthesis, such synthetic control is crucial, because the rates of intermolecular electron and energy transfer reactions depend strongly on distance. One needs to be able to fine-tune these rates, because they determine kinetic branching ratios for multi-step photochemical reactions. These branching ratios in turn determine the quantum efficiency of the overall photochemical process.

Numerous kinds of nanostructured and self-assembling systems, such as zeolites [1], clays [2], polymers [3], dendrimers [4], vesicles [5], and Langmuir–Blodgett films [6], have been studied as hosts for molecules that undergo light-induced energy and electron transfer reactions. Self-assembled inorganic multilayer films represent an interesting alternative to these [7]. They provide a simple and versatile route to complex thin film structures, which can be grown on both planar and high surface area substrates. The active components of these assemblies-photoactive transition metal complexes, organic dyes, and redox molecules-are confined to individual layers. Intermolecular distances are therefore quite well defined in the stacking direction, although there is little control over the structure in the lateral directions.

Earlier studies of artificial photosynthesis in inorganic thin films focused on the covalent attachment of one layer to the next, in most cases through metal–phosphonate linkages [8]. Recently, we have explored an alternative strategy, based on electrostatic self-assembly. This technique has a long history [9,10], but has only recently been applied to systems containing both organic and inorganic components [11–14]. The inorganic building blocks in this case are anionic sheets made by exfoliation of lamellar solids, such as α-zirconium phosphate (α-ZrP) or $HTiNbO_5$. The sheets separate polymer layers that contain the photo- and redox-active components of the system. Some important issues in this kind of assembly are the structural integrity of the organic/inorganic thin films, the reactivity of the edges of the sheets, and the participation of the inorganic 'spacer' in intramolecular electron transfer reactions. This paper reviews our recent work in this area, and presents some new data on the synthesis and properties of lamellar artificial photosynthetic systems.

2. Experimental

Microcrystalline and semicrystalline α-$Zr(HPO_4)_2 \cdot H_2O$ (α-ZrP), and microcrystalline $KTiNbO_5$, were synthesized and exfoliated as described previously [15,16]. Palladium(II)tetrakis (4-*N*,*N*,*N*-trimethylanilinium) porphyrin, chloride salt

($PdTAPP^{4+}$), and palladium(II)tetrakis(4-sulfonatophenyl) porphyrin, sodium salt ($PdTSPP^{4-}$) were used as received from Midcentury Chemicals. Poly(allylamine) hydrochloride, PAH, was derivatized at a loading of ca. 1/40–1/50 dye molecules per monomer unit by coupling the appropriate isothiocyanate or succinimidyl ester derivative of the dye (fluorescein or coumarin), as described in detail elsewhere [17]. The resulting Fl-PAH and Coum-PAH polymers were characterized by ^{1}H-NMR spectroscopy, elemental analysis, and gel permeation chromatography. The synthesis of ruthenium(polypyridyl) and viologen polycations, and the growth of multilayer films, is also described in detail elsewhere [17,18].

For fluorescent imaging of the edge chemistry of α-ZrP sheets, a phosphonated rhodamine B derivative (RhB-P) was prepared as follows: 17.2 mg rhodamine B isothiocyanate was dissolved in 20 ml DMF. 5.9 mg 3-(aminopropyl)phosphonic acid was dissolved in 20 ml water, and $NaHCO_3$ was added to a pH of 9.0. The two solutions were then combined and allowed to react for 3 h, in order to form a thiourea linkage. The solution was washed with hexane and diethyl ether, and the remaining solvent was then removed by rotary evaporation. The product solid was then washed with hot methanol. The edges of the α-ZrP sheets were derivatized by two methods. In one, self-assembled monolayers of α-ZrP on amine-primed borosilicate glass substrates were reacted for 2 h. at ambient temperature with a 1 μM aqueous solution of RhB-P. In the second, solid RhB–P was added to give approximately the same concentration in a 10 meq l^{-1} α-ZrP colloid. A sample of the colloidal sheets was obtained by dipping an amine-functionalized glass slide in the suspension for 10 min., followed by rinsing with water. In both cases the pattern of RhB–P adsorption was imaged using fluorescence microscopy.

3. Results and discussion

3.1. Synthesis and structure of multilayer thin films

Organic/inorganic multilayer films can be grown by a series of sequential adsorption reactions, as outlined in Fig. 1 [12]. The substrate, which is typically a glass slide or a non-porous silica particle, is primed with an aminoalkylsilane derivative. At neutral pH, the alkylammonium tail groups present a brush of positive charge to the solution. The suspended anionic α-ZrP sheets are charge-compensated by tetra(*n*-butylammonium) (TBA^+) cations, which are easily displaced by the higher charge density alkylammonium brush. A monolayer of sheets therefore adsorbs and tiles the surface densely; however, the adsorption process is self-limiting, because the surface charge is inverted in the adsorption process. The anionic α-ZrP-terminated surface can then adsorb a monolayer of polycations, and the two steps can be repeated as many times as desired to make a multilayer film.

Fig. 2 shows transmission electron micrographs (TEM) of hydrothermally synthesized silica colloids, exfoliated semicrystalline α-ZrP sheets, and the product of adsorbing the latter onto amine-derivatized silica. The unilamellar α-ZrP colloid consists of 50–100 nm diameter disk-like particles, which coat the surface of the silica. Histograms of silica particle sizes show that their average diameter increases

by about 2 nm, consistent with the thickness (ca. 0.8 nm) of the α-ZrP sheets. On planar substrates, monolayer and multilayer α-ZrP/polymer films have been characterized by ellipsometry, X-ray diffraction, atomic force microscopy (AFM), X-ray photoelectron spectroscopy, and near-field scanning optical microscopy (NSOM) [19–21]. The general picture that emerges from these studies is that layer growth occurs in stepwise fashion, and that the product thin film is structurally similar to bulk α-ZrP/polymer intercalation compounds of the same composition.

One of the important questions to ask about these lamellar thin films is whether the adsorption process really occurs one layer at a time. For related clay/polycation films, it appears that each adsorption step deposits about two monolayers of polymer or colloid. These then rearrange to give a single-stage intercalation compound on the surface [11]. X-ray and neutron diffraction studies show that in organic polyanion/polycation films, such as poly(styrenesulfonate)/PAH, there is also substantial mixing of layers [10]. These results do not augur well for artificial photosynthesis, for which electron donor–acceptor distances should be well defined. For α-ZrP/PAH films, however, the picture is different. Fluorescence

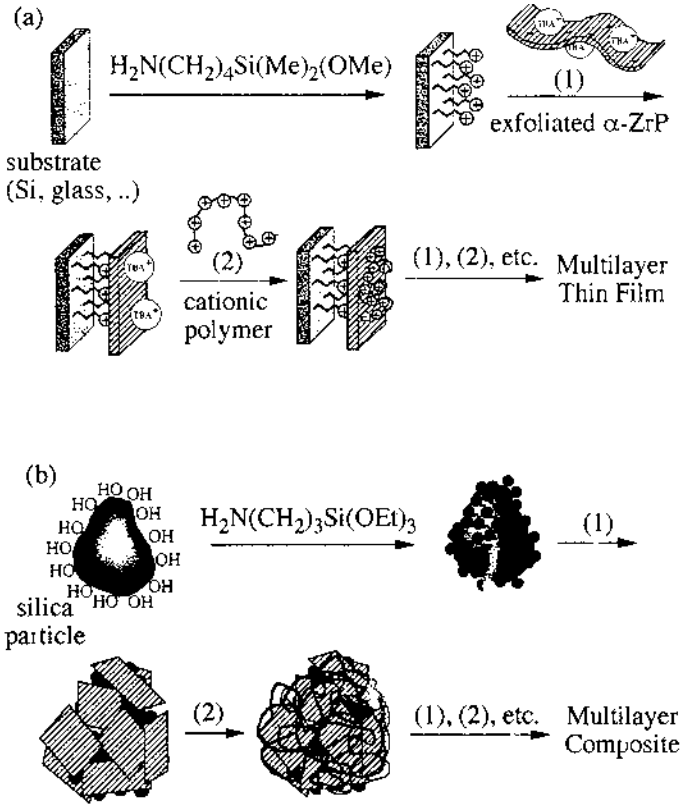

Fig. 1. Schematic representation of the sequential adsorption reactions of anionic α-ZrP sheets and cationic polymers on (a) planar and (b) high surface area substrates.

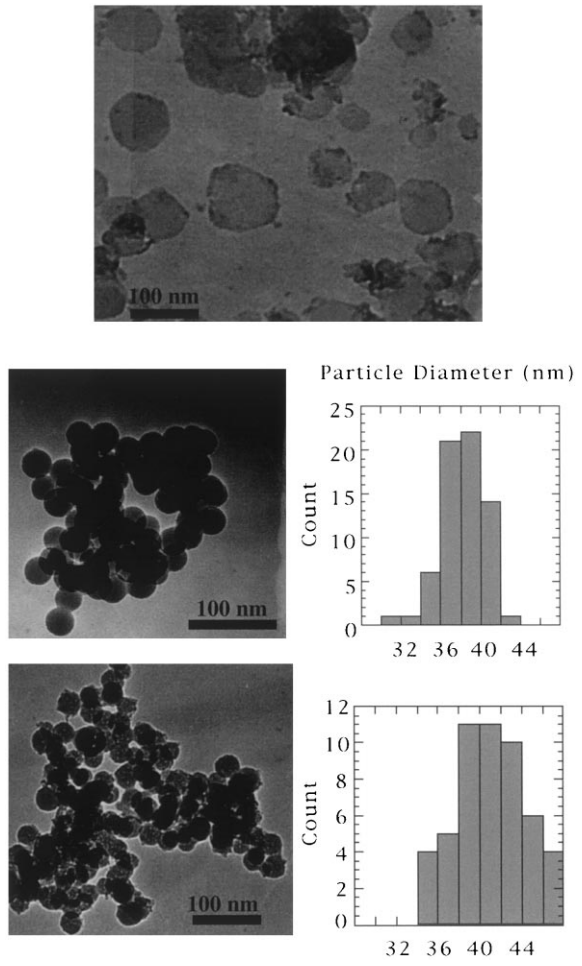

Fig. 2. Transmission electron micrographs of (top) exfoliated, semi-crystalline α-ZrP sheets, (center) silica particles, and (bottom) amine-primed silica coated by a single layer of sheets. Histograms of particle diameters before and after adsorption of α-ZrP are shown.

energy transfer between dye-PAH polymer strands has been used as a 'spectroscopic ruler,' to measure the degree of layer interpenetration. Experimental energy transfer efficiencies were compared with the results of Monte Carlo calculations for various sheet/polymer sequences [22]. These experiments show that there is essentially no 'shuffling' of PAH layers that are separated by α-ZrP sheets.

3.2. Edge chemistry of α-ZrP colloids

The base hydrolysis of α-ZrP, reaction (1), is an important side reaction that occurs in competition with exfoliation, reaction (2). Without proper precautions, the hydrolysis reaction can cause substantial corrosion of the sheets. The ultimate

$$Zr(HPO_4)_2 \cdot H_2O + nH_2O + 2xOH^- = Zr(HPO_4)_{2-x}(OH)_{2x} + (1+n)H_2O + xHPO_4^{2-} \quad (1)$$

$$Zr(HPO_4)_2 \cdot H_2O + xOH^- = [Zr(HPO_4)_{2-x}(PO_4)_x]^{x-} + xH_2O \quad (2)$$

product of base hydrolysis, hydrous zirconia, interferes with the layer adsorption process, resulting in incomplete surface coverage. AFM and TEM images of partially hydrolyzed sheets show that reaction (1) occurs from the edges inward [23]. The edges are more reactive than the basal plane surfaces, presumably because they contain phosphate groups that are bound to Zr atoms through two (or fewer) oxygen atoms. In contrast, the basal plane phosphates bind to Zr through three oxygen atoms [24].

There are two remedies for the hydrolysis reaction. The first takes advantage of the fact that reaction (1) has a higher activation energy than (2). By carrying out the exfoliation at 0°C, hydrolysis-free colloids can be obtained. The second strategy is to use Le Chatelier's principle to drive reaction (1) in reverse. The addition of phosphate, the product of reaction (1), slows the reaction without affecting the rate of (2). Interestingly, the same mass action principle can be used to derivatize the edges of the sheets selectively, by adding phosphonic acids. Fig. 3 compares electron micrographs of microcrystalline α-ZrP colloids, which were exposed to conditions (22°C, pH 10.5–11) that promote hydrolysis in the absence of added phosphate or phosphonate. In one sample, vinylphosphonic acid was added to prevent hydrolysis, and in the other ethylphosphonic acid was used. OsO_4 was then added to both suspensions. In the sample containing vinylphosphonic acid, exchange for phosphate groups leaves particles with vinyl groups at the edges. These then react with OsO_4 to make colloids of osmium(IV) oxide, which decorate the edges of the sheets. In the ethylphosphonate sample, exchange of phosphonate for

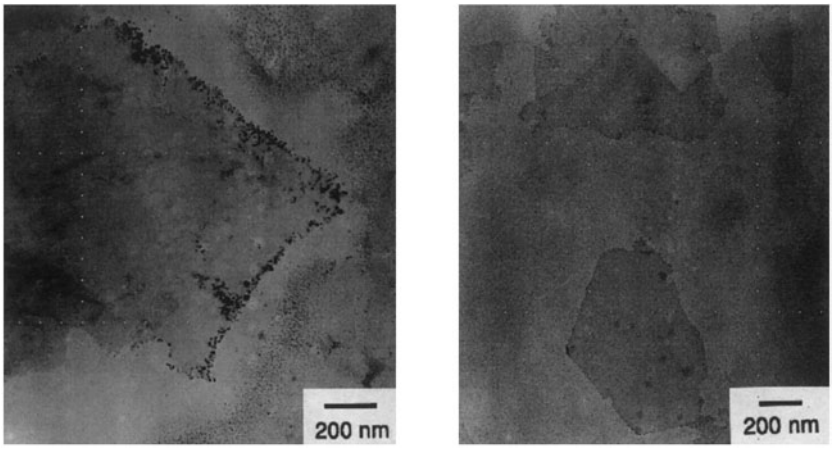

Fig. 3. TEM images of exfoliated microcrystalline α-ZrP, reacted with vinylphosphonic acid and OsO_4 (left) and with ethylphosphonic acid and OsO_4 (right).

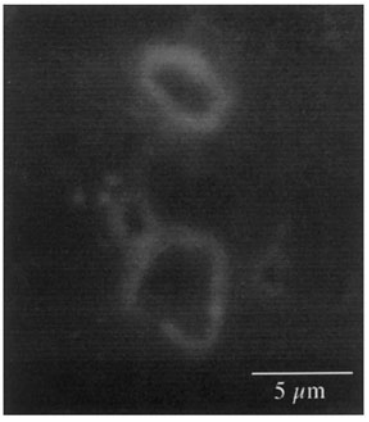

Fig. 4. Fluorescence microscope image of α-ZrP sheets derivatized at the edges with RhB-P, on a borosilicate glass cover slip.

edge phosphate again prevents corrosion of the sheets. However, these edges lack olefinic groups and therefore do not bind osmium oxide. While osmium oxide colloidal particles are also found in this sample, they are not associated with either the edges or basal planes of the α-ZrP sheets.

The same phosphonate-phosphate exchange reaction can be used to place dye molecules exclusively at the edges of the sheets, either in a self-assembled monolayer or in a colloidal suspension. Fig. 4 shows fluorescence microscope images of a partial monolayer of α-ZrP on glass, which was exposed to an aqueous RhB–P solution and then rinsed with water to remove excess dye. The particles show the characteristic red luminescence of RhB, and the loop patterns are consistent with selective edge binding. Control experiments with RhB derivatives that contain no phosphonate group do not show edge luminescence.

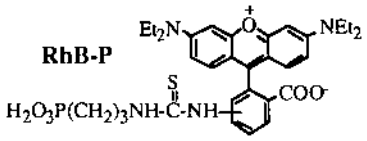

3.3. Photoinduced electron transfer

The α-ZrP sheets provide a 0.8 nm thick, insulating spacer layer between polycation layers. In order to study photoinduced electron transfer across these sheets, polycations containing pendent $Ru(bpy)_3^{2+}$ and viologen groups were synthesized. The $Ru(bpy)_3^{2+}$/viologen dyad has been well studied in solution and in several kinds of supramolecular systems [1–5]. Photoexcitation makes a metal-to-ligand charge transfer (MLCT) state, which can be quenched by electron transfer to the viologen electron acceptor. With high surface area composites of the type

shown in Fig. 1, a photoredox 'onion' can be grown by sequentially adsorbing viologen, α-ZrP, and $Ru(bpy)_3^{2+}$ layers onto amine-derivatized silica. In this simple dyad, there is no quenching of the $Ru(bpy)_3^{2+}$ MLCT excited state by viologen molecules in the inner layer [25]. Apparently, the modest driving force of this reaction (ca. 0.28 V) is not sufficient for electron transfer on the timescale of the MLCT state (600 ns), over the relatively long donor–acceptor distance imposed by the α-ZrP sheets. However, addition of the anionic electron donor p-methoxyanilinedi(ethylsulfonate), MDESA, to the suspension causes efficient MLCT state quenching. The reduced $Ru(bpy)_3^{+}$ complex generated in this process is a substantially stronger reducing agent than MLCT state $Ru(bpy)_3^{2+}$, and consequently rapid reduction of the viologen polymer occurs across the α-ZrP layer. Fig. 5 summarizes the sequence of electron transfer steps that occur in this system. Photoexcitation of the $Ru(Me\text{-}vpby)(bpy)_2^{2+}$ polymer results two forward electron transfer reactions, which are too fast to measure on the instrumental timescale (≤ 50 ns). The reduced viologen-oxidized MDESA charge separated state is evidenced by transient absorbance peaks at 390 and 550–600 nm, which are characteristic of the intensely colored viologen cation radical, and a 510 nm transient from oxidized MDESA [18,25]. This charge separated state is relatively long lived ($\tau \approx 40$ μs), because the back reaction must occur across a $Ru(bpy)_3^{2+}$ polymer layer and a layer of α-ZrP sheets.

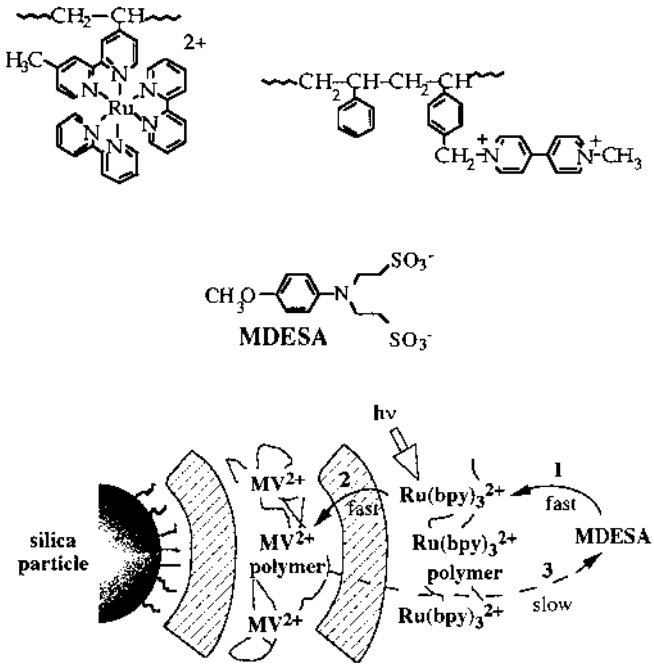

Fig. 5. Schematic representation of the $Ru(bpy)_3^{2+}$/α-ZrP/viologen 'onion' structure grown on colloidal silica particles. The sequence of fast (1, 2) and slow (3) electron transfer steps that follow photoexcitation of the $Ru(Me\text{-}vpy)(bpy)_2^{2+}$ polymer is shown.

3.4. Multicomponent energy/electron transfer cascades

In natural photosynthesis, most of the chromophoric molecules have a light harvesting function, and relatively few are involved in electron transfer reactions. The light harvesting complexes consist of symmetric bundles of energy donors and acceptors, which efficiently funnel excitation to the reaction centers where electron transfer occurs [26]. Mimicking this combined energy/electron transfer cascade is a worthy challenge, which has been met in several artificial photosynthetic systems [27]. Most of these studies have involved making supermolecules, in which different subunits (energy and electron donors and acceptors) are linked together covalently. Inorganic self-assembly represents a synthetically simple alternative for preparing such multifunctional assemblies. In principle, very large and complex structures can be made by simply stacking the appropriate components on top of each other.

Fig. 6 illustrates the design of a multilayer film that consists of a three-chromophore light harvesting layer, separated by an inorganic spacer from an electron acceptor layer. The three chromophores (fluorescein, coumarin, porphyrin) were chosen to maximize spectral overlap between donor emission and acceptor absorbance, and also to maximize the quantum yield of interlayer electron transfer. The coumarin and fluorescein molecules are covalently bound at low loading (1/40–1/50 per monomer unit) to PAH. These polymers (Coum-PAH and Fl-PAH) are then coadsorbed with either a cationic or anionic porphyrin ($PdTAPP^{4+}$ or $PdTSPP^{4-}$). In the case of $PdTAPP^{4+}$, all three cations are adsorbed simultaneously, and in the case of $PdTSPP^{4-}$, a cation-anion-cation (Coum-PAH, $PdTSPP^{4-}$, Fl-PAH) sequence is used.

Fig. 7 shows representative emission spectra for the simple coumarin-fluorescein-porphyrin triad, and for a similar system containing a viologen electron acceptor layer. The triad spectra (top) were obtained by exciting into the absorption band of the coumarin primary donor, at 450 nm. The figure shows reference spectra of coumarin and fluorescein monolayers, which have broad emission maxima centered at 485 and 530 nm, respectively. The porphyrin energy acceptor has very little emission across the visible region when excited at 450 nm, because it absorbs only weakly there. However, when the three dyes are combined in a single layer, both the coumarin and fluorescein emission are substantially quenched. Phosphorescence is observed at 720 nm, indicating energy transfer to the porphyrin. By deconvoluting these steady state emission spectra, it is possible to determine the quantum yield for the Coum → Fl → porphyrin energy transfer process, which is about 80% overall.

When a viologen polymer layer is added to this particular assembly, there is no electron transfer quenching of the porphyrin triplet state, because of the relatively weak driving force ($\Delta G^{\circ} \approx +0.05$ eV) for the reaction. However, the assembly shown at the bottom of Fig. 7 contains the anionic porphyrin $PdTSPP^{4-}$, which is a stronger triplet state reducing agent, by 0.3 eV, than $PdTAPP^{4+}$ [28]. In this case the electron transfer reaction does occur, as indicated by the disappearance of the porphyrin phosphorescence. Again, one may deconvolute the spectra to calculate an overall quantum yield for the four-component energy/electron transfer cascade, which in this case is 47%. Interestingly, when an $HTiNbO_5$ spacer layer is

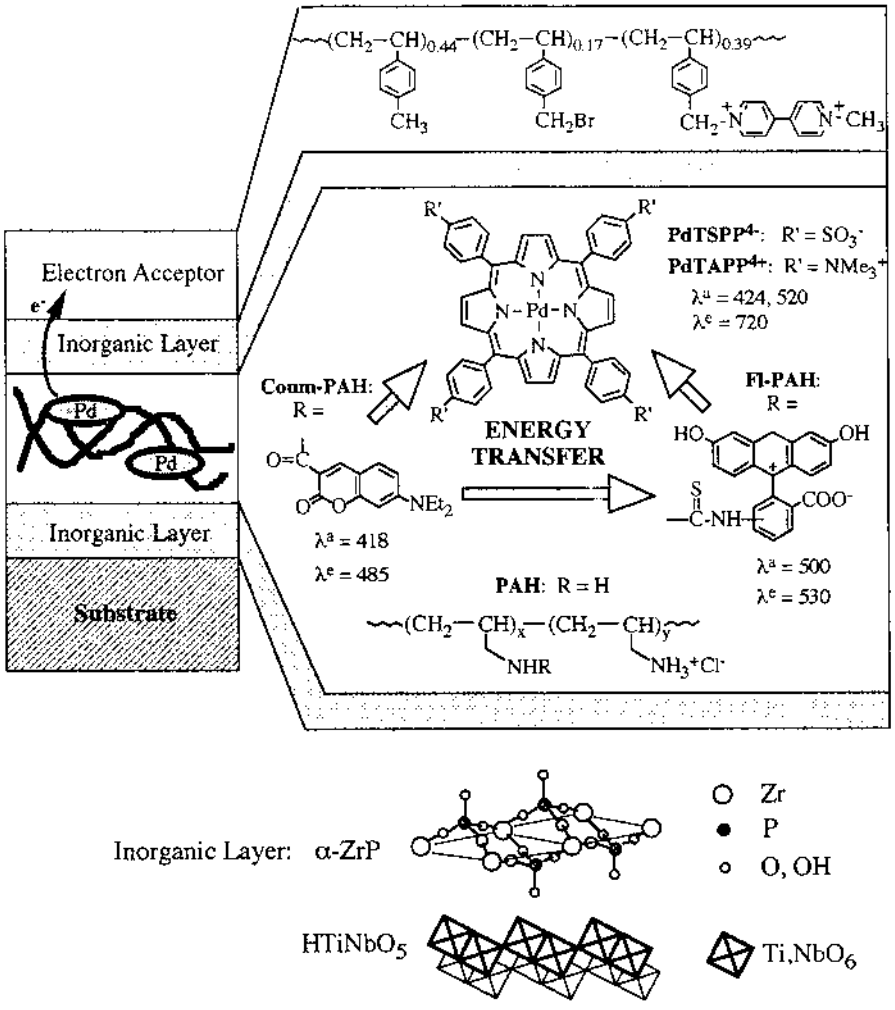

Fig. 6. Schematic drawing of a multilayer film containing a coumarin-fluorescein-porphyrin light-harvesting layer, and a viologen electron acceptor layer separated by an inorganic spacer (α-ZrP or $HTiNbO_5$).

substituted for α-ZrP, the same assembly has a substantially higher quantum yield (61%) for the combined energy/electron transfer process.

While steady-state emission spectra provide some information about the energy transfer process and the porphyrin → viologen electron transfer reaction, they are not informative about the nature or lifetime of the charge separated state. Transient spectra, acquired from high surface area samples, provide useful information on these points, and also highlight the difference between the two kinds of inorganic spacer layers. Fig. 8 shows transient spectra acquired 200 μs after a 532 nm laser flash, for porphyrin/spacer (α-ZrP or $HTiNbO_5$)/viologen samples. The spectra

clearly show the signature of the reduced viologen (maxima at 380 and 600 nm). The extinction coefficient of the oxidized porphyrin is too small for the latter to be observed. The inset shows the transient decay of the charge separated state, monitored at 600 nm. There is again a striking difference between the two kinds of spacers. While the α-ZrP-containing sample shows a first-order decay with a lifetime of 150 μs, the decay with the $HTiNbO_5$ spacer is biexponential, and there is a substantial component with a much longer (900 μs) lifetime.

The difference in charge separation quantum yields and charge recombination kinetics is unlikely to arise from simple geometric factors, since the α-ZrP and $HTiNbO_5$ spacers have about the same thickness. A more plausible explanation is that the semiconducting $HTiNbO_5$ spacers play an active role in the reaction, by mediating electron transfer between the porphyrin and viologen. In support of this hypothesis, there is significant quenching of the porphyrin excited state in the absence of viologen by $HTiNbO_5$, but not by α-ZrP, which is an electronic insulator. The conduction band of the semiconductor has electronic states that are

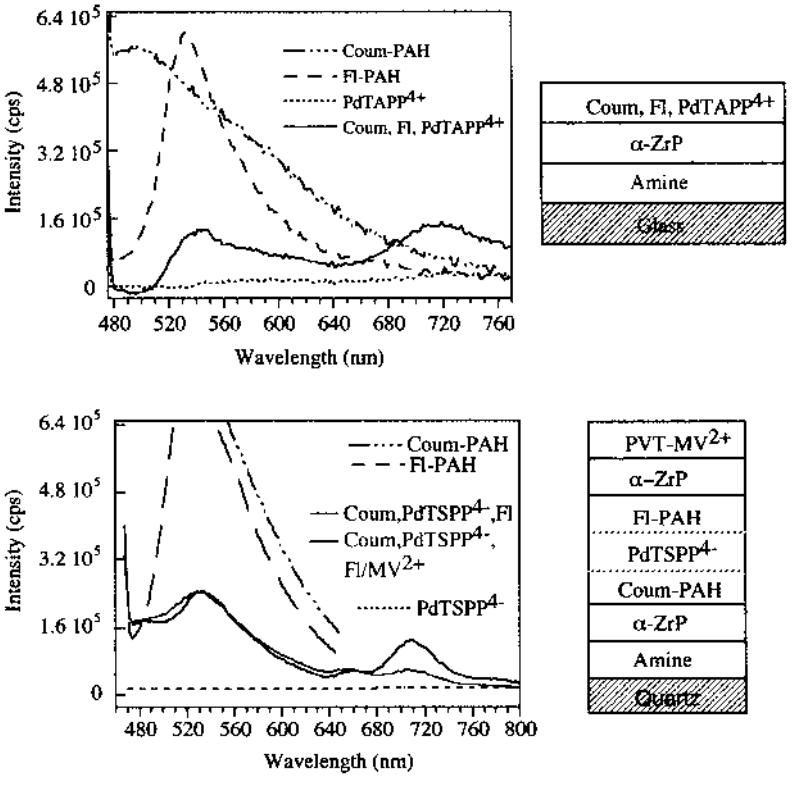

Fig. 7. Top: Steady state emission spectra ($\lambda_{ex} = 450$ nm) of adsorbed monolayers of Coum-PAH and Fl-PAH polycations, $PdTAPP^{4+}$, and the co-adsorbed coumarin-fluorescein-porphyrin triad. Bottom: emission spectra of a similar triad containing $PdTSPP^{4-}$, with and without an added viologen electron acceptor layer.

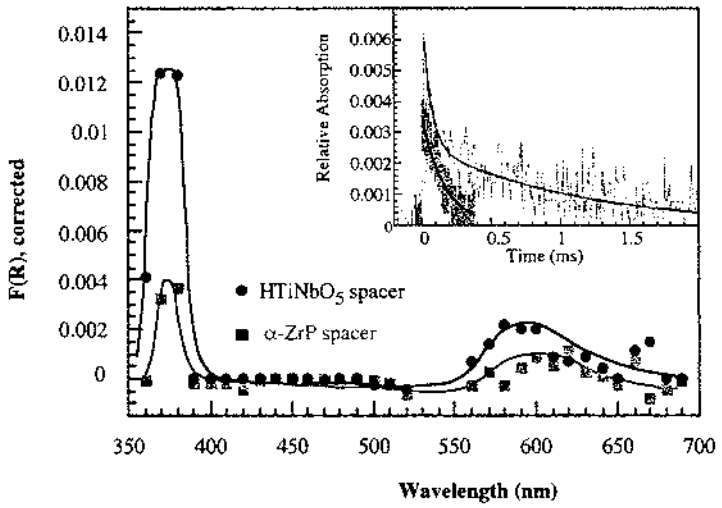

Fig. 8. Transient diffuse reflectance spectra taken 200 μs after 532 nm, 15 ns laser excitation of a silica suspension with the layer sequence amine/α-ZrP/polyviologen/spacer/PAH/$PdTSPP^{4-}$ (spacer = α-ZrP or $HTiNbO_5$). Inset shows transient decays at 600 nm; the upper trace was obtained from a sample with a $HTiNbO_5$ spacer layer, and the upper trace with α-ZrP

intermediate in energy between the porphyrin and viologen redox levels; however, these states cannot participate in the back electron transfer reaction, which involves more the more positive ground-state redox level of the porphyrin.

4. Conclusions

Self-assembly provides a means of growing polymer/inorganic sheet intercalation compounds on surfaces, one layer at a time. The basal planes and edges of the inorganic sheets have distinctly different chemistry, and their selective reactions can be exploited to make either stacked or edge-decorated structures. Because different photoactive and redox-active components can be placed in successive layers, the layer-by-layer assembly technique provides a synthetically easy and useful route to complex structures, which combine the functions of light harvesting and electron transfer. Hopefully, these studies may be extended in the future to useful photoconversion systems, by coupling the electron transfer reactions to the appropriate catalytic centers or to an external circuit. These possibilities will be investigated in future experiments.

Acknowledgements

This work was supported by the Division of Chemical Sciences, Office of Basic Energy Sciences, Department of Energy, under contract DE-FG02-93ER14374. We

thank Dr Mary Kunze of the Center for Quantitative Cell Analysis, Pennsylvania State University, for assistance with the fluorescence microscopy experiments.

References

[1] (a) L.R. Faulkner, S.L. Suib, C.L. Renschler, J.M. Green, P.R. Bross, in: Chemistry in Energy Production, Wiley, New York, 1982, pp. 99–114. (b) P.K. Dutta, J.A. Incavo, J. Phys. Chem. 91 (1987) 4443. (c) J.S. Krueger, J.E. Mayer, T.E. Mallouk, J. Am. Chem. Soc. 110 (1988) 8232. (d) J.A. Incavo, P.K. Dutta, J. Phys. Chem. 94 (1990) 3075. (e) S. Sankaraman, K.B. Yoon, T. Yake, J. Kochi, J. Am. Chem. Soc. 113 (1991) 1419. (f) P.K. Dutta, W. Turbeville, J. Phys. Chem. 96 (1992) 5024. (g) P.K. Dutta, W. Turbeville, J. Phys. Chem. 96 (1992) 9410. (h) K. Maruszewski, D.P. Strommen, J.R. Kincaid, J. Am. Chem. Soc. 115 (1993) 8345. (i) E.H. Yonemoto, Y.I. Kim, R.H. Schmehl, J.O. Wallin, B.A. Shoulders, B.R. Richardson, J.F. Haw, T.E. Mallouk, J. Am. Chem. Soc. 116 (1994) 10557. (j) M. Ledney, P.K. Dutta, J. Am. Chem. Soc. 117 (1995) 7687. (k) M. Sykora, K. Maruszewski, S.M. Treffert-Ziemelis, J.R. Kincaid, J. Am. Chem. Soc. 120 (1998) 3490.

[2] A.J. Bard, T.E. Mallouk, Molecular Design of Electrode Surfaces, Wiley, New York, 1992, pp. 271–312.

[3] (a) J.K. Whitesell, H.K. Chang, M.A. Fox, E. Galoppni, D.M. Watkins, H. Fox, B. Hong, Pure Appl. Chem. 68 (1996) 1469. (b) C.A. Slate, D.R. Striplin, J.A. Moss, P. Chen, B.W. Erickson, T.J. Meyer, J. Am. Chem. Soc. 120 (1998) 4885.

[4] (a) V. Balzani, S. Campagna, G. Denti, A. Juris, S. Serroni, M. Venturi, Acc. Chem. Res. 31 (1998) 26. (b) G.M. Stewart, M.A. Fox, J. Am. Chem. Soc. 118 (1996) 4354.

[5] J(a) .K. Hurst, D.H.P. Thompson, J.S. Connolly, J. Am. Chem. Soc. 109 (1987) 507. (b) B.C. Patterson, D.H. Thompson, J.K. Hurst, J. Am. Chem. Soc. 110 (1988) 3656.

[6] (a) H. Kuhn, J. Chem. Phys. 53 (1970) 101. (b) P. Fromherz, W. Arden, Ber. Bunsenges. Phys. Chem. 84 (1980) 2045. (c) M. Fujihira, in: Photochemical Processes in Organized Molecular Systems, North-Holland, Amsterdam, 1991.

[7] (a) G. Cao, H.-G. Hong, T.E. Mallouk, Acc. Chem. Res. 25 (1992) 420. (b) T.E. Mallouk, H.-N. Kim, P.J. Ollivier, S.W. Keller, in: Comprehensive Supramolecular Chemistry, Vol. 7, Elsevier, Oxford, 1996, pp. 189–217.

[8] (a) H. Byrd, E.P. Suponeva, A.B. Bocarsly, M.E. Thompson, Nature, 380 (1996) 610. (b) W.L. Wilson, H.E. Katz, G.R. Scheller, T.M. Putvinski, J. Am. Chem. Soc. 114 (1992) 8717.

[9] R.K. Iler, J. Colloid Interface Sci. 21 (1966) 569.

[10] G. Decher, Science 277 (1997) 1232, and references therein.

[11] (a) E.R. Kleinfeld, G.S. Ferguson, Science, 265 (1994) 370. (b) E.R. Kleinfeld, G.S. Ferguson, Chem. Mater. 7 (1995) 2329.

[12] S.W. Keller, H.-N. Kim, T.E. Mallouk, J. Am. Chem. Soc. 116 (1994) 8817.

[13] Y. Lvov, K. Ariga, T. Kunitake, J. Am. Chem. Soc. 117 (1995) 6117.

[14] N.A. Kotov, I. Dekany, J.H. Fendler, Adv. Mater. 8 (1996) 637.

[15] M.E. Garcia, J.L. Naffin, N. Deng, T.E. Mallouk, Chem. Mater. 7 (1995) 1968.

[16] G.B. Saupe, W. Kim, R.H. Schmehl, T.E. Mallouk, J. Phys. Chem. B 101 (1997) 2491.

[17] D.M. Kaschak, J.T. Lean, C.C. Waraksa, G.B. Saupe, T.E. Mallouk, J. Am. Chem. Soc. 121 (1999).

[18] S.W. Keller, S.A. Johnson, E.H. Yonemoto, E.S. Brigham, G.B. Saupe, T.E. Mallouk, in Photochemistry and Radiation Chemistry: Complementary Methods for the Study of Electron Transfer, Vol. 254, Adv. Chem. Ser. 1998, pp. 359–379.

[19] H.-N. Kim, S.W. Keller, T.E. Mallouk, J. Schmitt, G. Decher, Chem. Mater. 9 (1997) 1414.

[20] M. Fang, D.M. Kaschak, A.C. Sutorik, T.E. Mallouk, J. Am. Chem. Soc. 119 (1997) 12184.

[21] J. Kerimo, D. Adams, D.M. Kaschak, P.F. Barbara, T.E. Mallouk, J. Phys. Chem. B 102 (1998) 9451.

[22] D.M. Kaschak, T.E. Mallouk, J. Am. Chem. Soc. 118 (1996) 4222.
[23] D.M. Kaschak, S.A. Johnson, D.E. Hooks, H.-N. Kim, M.D. Ward, T.E. Mallouk, J. Am. Chem. Soc. 120 (1998) 10887.
[24] (a) G. Alberti, Acc. Chem. Res. 11 (1978) 163. (b) A. Clearfield, Chem. Rev. 88 (1988) 125.
[25] S.W. Keller, S.A. Johnson, E.H. Yonemoto, E.S. Brigham, T.E. Mallouk, J. Am. Chem. Soc. 117 (1995) 12879.
[26] R. Huber, Angew. Chem. Int. Ed. Engl. 28 (1989) 848.
[27] (a) D. Gust, T.A. Moore, A.L. Moore, Acc. Chem. Res. 26 (1993) 198. (b) M.R. Wasielewski, Chem. Rev. 92 (1992) 435.
[28] A. Harriman, M. Richoux, P. Neta, J. Phys. Chem. 87 (1983) 4957.